

# LA-UR-13-23011

Approved for public release; distribution is unlimited.

Title: Fiber Bragg Grating Sensing of Detonation and Shock Experiments at Los Alamos National Laboratory

Author(s): Rodriguez, George  
Sandberg, Richard L.  
Jackson, Scott I.  
Dattelbaum, Dana M.  
Vincent, Samuel W.  
McCulloch, Quinn  
Martinez, Ricardo M.  
Gilbertson, Steve M.  
Udd, Eric

Intended for: SPIE Defense, Security, and Sensing 2013 - Fiber Optic Sensing and Applications X, 2013-04-29/2013-05-03 (Baltimore, Maryland, United States)

Issued: 2013-04-26



**Disclaimer:**

Los Alamos National Laboratory, an affirmative action/equal opportunity employer, is operated by the Los Alamos National Security, LLC for the National Nuclear Security Administration of the U.S. Department of Energy under contract DE-AC52-06NA25396. By approving this article, the publisher recognizes that the U.S. Government retains nonexclusive, royalty-free license to publish or reproduce the published form of this contribution, or to allow others to do so, for U.S. Government purposes. Los Alamos National Laboratory requests that the publisher identify this article as work performed under the auspices of the U.S. Department of Energy. Los Alamos National Laboratory strongly supports academic freedom and a researcher's right to publish; as an institution, however, the Laboratory does not endorse the viewpoint of a publication or guarantee its technical correctness.

# Fiber Bragg grating sensing of detonation and shock experiments at Los Alamos National Laboratory

G. Rodriguez\*<sup>a</sup>, R. L. Sandberg<sup>a</sup>, S. I. Jackson<sup>a</sup>, D. M. Dattelbaum<sup>a</sup>,  
S.W. Vincent<sup>a</sup>, Q. McCulloch<sup>a</sup>, R. M. Martinez<sup>a</sup>, S. M. Gilbertson<sup>a</sup>, and E. Udd<sup>b</sup>

<sup>a</sup>Los Alamos National Laboratory, P.O. Box 1663, Los Alamos, NM, USA 87545-3502;

<sup>b</sup>Columbia Gorge Research, PO Box 382, 2555 NE 205th Ave., Fairview, OR USA 97024

## ABSTRACT

An all optical-fiber-based approach to measuring high explosive detonation front position and velocity is described. By measuring total light return using an incoherent light source reflected from a fiber Bragg grating sensor in contact with the explosive, dynamic mapping of the detonation front position and velocity versus time is obtained. We demonstrate two calibration procedures and provide several examples of detonation front measurements: PBX 9502 cylindrical rate stick, radial detonation front in PBX 9501, and PBX 9501 detonation along a curved meridian line. In the cylindrical rate stick measurement, excellent agreement with complementary diagnostics (electrical pins and streak camera imaging) is achieved, demonstrating accuracy in the detonation front velocity to below the 0.3% level when compared to the results from the pin data. In a similar approach, we use embedded fiber grating sensors for dynamic pressure measurements to test the feasibility of these sensors for high pressure shock wave research in gas gun driven flyer plate impact experiments. By applying well-controlled steady shock wave pressure profiles to soft materials such as PMMA, we study the dynamic pressure response of embedded fiber Bragg gratings to extract pressure amplitude of the shock wave. Comparison of the fiber sensor results is then made with traditional methods (velocimetry and electro-magnetic particle velocity gauges) to gauge the accuracy of the approach.

**Keywords:** fiber Bragg grating sensors, high explosive diagnostics, detonation, shock physics, pressure measurements

## 1. INTRODUCTION

In the performance characterization of high explosives (HE), the measurement of detonation wave speed is a fundamental quantity obtained through experimentation for comparison to equation-of-state models and hydrodynamic simulations that accurately predict detonation propagation, energy delivery, and timing. In addition to HE detonation velocity, there is also critical need for *in-situ* probes that can continuously measure thermodynamic state variables (*i.e.*, pressure and temperature) under several critical geometries important for high explosive and shock wave science. Problems of interest range from new formulation burn rates, surety engineering, initiation systems, to complex propagation in confined geometries with multiple material boundaries. These quantities (velocity, pressure, and temperature) are used to model the detonation and shock wave evolution through a system along with subsequent detonation product and inert confiner motion.<sup>1,2</sup> For well over fifty years, elaborate methods have been used for measuring detonation and shock arrival positions including electrical shorting pins, ionization pins, piezoelectric gauges, and more recently fiber optic probes and microwave strip lines because of their reliability, time and position accuracy, and ease of use.<sup>3-6</sup> Yet they still retain certain drawbacks in their use that pertain to high voltage safety in proximity to high explosives, multiplexing recording channels, and discretization of data time signals when a continuous record is desired. Other approaches of detonation or shock velocity measurement is done using surface probes (VISAR, photonic Doppler velocimetry (*i.e.* PDV), high speed optical camera imaging), discreet embedded gauges (pins, strain gauges), material density probes (x-rays, proton radiography), or low density flow fields with particle imaging velocimetry (*i.e.* PIV). Even the latest velocimetry PDV approaches using embedded fiber probes in explosives<sup>7</sup> require careful light collection matching using bare PDV single-mode fiber with a liquid waveguide surrounding the fiber that is buffered with a 1.6 mm diameter Teflon tube. In these probes, great care is taken to make sure that the light rays reflected off the detonation front and collected by the embedded PDV probe are parallel to the detonation front propagation to prevent loss of return light signal. Additionally the large size of the embedded probe is also undesirable from a modeling perspective due to possible detonation flow disruption.

\*rodrigeo@lanl.gov; phone 1 505 665-3408; fax 1 505 665-9030

Alternatively, embedded sensors based on single mode fiber Bragg gratings (FBG) offer an attractive alternative means for measuring dynamic events such as shock and detonation due to their compact diameter ( $\sim 125 \mu\text{m}$ ), flexibility in placement, and ease of use with standard recording equipment that is less stringent than, say, PDV based systems. A FBG consists of a periodic variation in the index of refraction in the core of an optical fiber which acts as a distributed reflector. The light traveling down the fiber optic is reflected back towards its source by interacting with the modulated index of refraction. In the case of a full blown detonation, the FBG detonation wave velocity sensor relies on a time sequenced destruction of the FBG by the detonation front. However, we have also begun to explore possible use of the sensor under conditions when the probe is not instantaneously destroyed by a propagating detonation front, such as in situations where a high pressure shockwave interacts with the FBG in regimes where the FBG is believed to retain its mechanical integrity.<sup>8-10</sup> Because FBGs sensors have predictable pressure and thermo-mechanical response properties,<sup>10,11</sup> the prospect of using FBGs for measuring high pressure (and temperature) under dynamic loading or explosive conditions is attractive. Recent successful experiments by Udd, *et al.*<sup>11,12</sup> in deflagrating explosives have shown this to be the case, where success in measuring pressure and temperature in deflagration-to-detonation (DDT) RDX explosive pipe tests to  $\geq 80$  kbar and  $400^\circ\text{C}$  were reported. His results are significant in that the embedded FBG approach appears to measure the *in situ* dynamic conditions where gradients from violent HE chemical reactions result in extreme temperature and pressure conditions under multiple “burn” environments: ignition, slow cook-off, deflagration, and detonation. The results are impressive, and technique is still under developmental testing.

At Los Alamos, we have applied the technology to develop a diagnostic baseline for both HE detonation velocity and shock pressure measurements. In the HE detonation case, we seek to establish confidence levels in the approach by performing measurements that try to determine precision and response speeds. The HE detonation measurements we report here are aimed at demonstrating precision by comparing with complementary diagnostics, and are also aimed at determining response times by making measurements in cases where the detonation velocity is expected to vary, such as in a situation where multiple explosives are used or when the velocity is changing as the detonation propagates with a varying phase velocity due to geometry of the burn path. We also aim at testing FBGs where the total burn distances are long, *i.e.*, tens of centimeters. In Section 2, we describe HE detonation velocity measurements using FBGs in several experiments: linear rate stick, a multi-HE linear rate stick, and detonation along a curvilinear surface. In the case of shock pressure measurements, our aim was to complement development of HE DDT pressure and temperature measurements by concentrating on pressure-only dynamic systems. That is, to demonstrate design principles, technique, and proof-of principle measurements on flyer-target impact plate experiments where the pressure state in the target is well defined and unfolding of data is less complex than DDT measurements. We believe that this complementary approach is reasonable to allow for a graded FBG sensor development from low to high pressures. In Section 3, we report on preliminary FBG pressure studies using a single-stage gas gun driven flyer plate impact station. We demonstrate results for experiments to 14 kbar, and describe a path forward for FBG probe detection changes that are under development at the time of this manuscript preparation.

## 2. HIGH EXPLOSIVE DETONATIONS

### 2.1 Methodology

Based on pioneering development work by Benterou and Udd<sup>11-14</sup> we explored the use of embedded fiber optic sensors using linearly chirped fiber Bragg gratings (CFBG) for detonation front measurement experiments under several HE geometries that demonstrated the technique’s versatility.<sup>15-17</sup> Here we briefly describe the approach, review our previous results, and report on new measurements.

Our detonation velocity detection system is described in detail elsewhere<sup>15</sup> and we give a brief description here. A block diagram of the experimental setup is shown in Figure 1. We used an incoherent broadband amplified spontaneous emission (ASE) source centered about the well-known telecommunication C-band (1525 nm - 1565 nm). Light from the ASE light source is launched into a single-mode fiber system to a 3-port power circulator. The power circulator directs light to the embedded CFBG sensor. The CFBG sensor consists of a linearly chirped grating written along a predetermined length of bare SMF-28 with maximum reflectivity within the C-band. Detonation wave sensing is accomplished with the sensor by being in direct contact (embedded or surface) with the HE. As the HE detonation wave travels along the length of the sensor, the fiber’s index of refraction is first modified by the intense shock driven into the fiber by the adjacent high-pressure detonation products as the wave propagates axially along the grating’s length. In rapid succession, the grating is consumed by the high temperatures and pressures associated with this event. Shock-

processed portions of the grating no longer transmit/reflect light due to substantial modification to the local index of refraction and damage of the grating structure. Since spectral encoding of the CFBG wavelength reflection band is linear with length (linear chirp), propagation of a detonation axially along the fiber grating continually and linearly reduces the reflected grating bandwidth as a function of time. Thus, the detonation phase velocity along the fiber axis can be measured by a CFBG embedded in the HE or placed at various boundaries able to accommodate the bare 150- $\mu\text{m}$ -diameter fiber (125  $\mu\text{m}$  for cladding with 25  $\mu\text{m}$  of recoating, typically polyamide). For our experiments, power levels launched into the CFBG detonation velocimetry system were typically 0.0 dBm (1 mW). Near complete total reflection ( $> 90\%$  light return) off the CFBG occurs along the detection leg of the system. After reflecting off the CFBG, the reflected light is directed through the power circulator at port 2, where only reflected light off the CFBG is detected at the circulator output port (port 3) using a fast (250 MHz BW) InGasAs photodetector (Timbercon, Inc.). Dynamic recording of the event is done with a fast recording digitizing oscilloscope. The current bandwidth of the measurement system is limited by the response time of the photodiode.

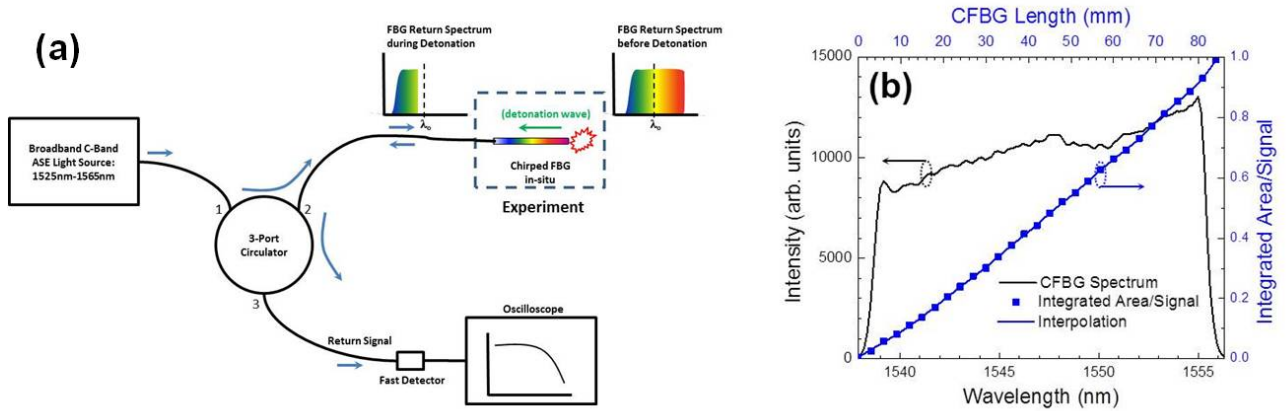


Figure 1. (a) Chirped fiber Bragg (CFBG) detonation detection system, and (b) an example showing the spectrum of an 85-mm long CFBG sensor. The blue square symbol-line plot is the integrated area plot of the CFBG power as a function of length (wavelength) according to Equation 1.

Transformation from the experimentally recorded trace of voltage versus time at the detector is related to the length/position versus time response function of the grating after data reduction. The grating reflection bandwidth is centered at 1550 nm, but is less than the bandwidth of the ASE light source so that the flattest spectral portion of the ASE source overlaps with the grating reflectance band. The reflected intensity,  $R$ , is proportional to the integrated return light spectrum off the grating. However, since encoding of grating length versus wavelength is linear,  $R$  is linearly proportional to  $L$  and  $\lambda$ , provided that the grating reflected spectrum produced by the ASE light source can be assumed to be an idealized flat-top. In general, the integrated light return voltage signal is,<sup>13,14</sup>

$$R(t) = a \int_{\lambda_1}^{\lambda_2(t)} S_G(\lambda) ASE(\lambda) d\lambda \quad (1)$$

where,  $a$  is a normalization constant,  $S_G(\lambda)$  is the grating reflection spectrum,  $ASE(\lambda)$  is the light source spectrum, and  $\lambda_1$  and  $\lambda_2$  are the lower and upper wavelength limits, respectively. Here we assume  $\lambda_2$  is the wavelength position where the detonation wave is located, *i.e.*,  $L(t) \propto R(t)$ , and  $\lambda_1$  corresponds to the shortest wavelength reflected by the grating, which is located nearest to the light source. We also assume that the photodiode has a flat spectral response across the CFBG reflectance band. Data analysis yields time-of-arrival data  $L(t)$  for a detonation propagating along the CFBG sensor. The temporal derivative of  $L(t)$  computes the local detonation phase velocity along the fiber.

## 2.2 PBX 9502 Linear Rate Stick

A cylindrical rate stick measurement of the insensitive HE PBX 9502 (95 wt.% TATB, 5 wt.% Kel-F 800) was performed. The experimental geometry consisted of a 157.08-mm-long, 16.3-mm-diameter PBX 9502 cylindrical rod that was boosted by a 12.7-mm-diameter and 12.7-mm-long PBX 9407 booster pellet (94 wt.% RDX, 6 wt.% FPC461) and initiated by an RP-1 detonator (Teledyne RISI, Inc.) as shown in Figure 2. The test was equipped with two CFBG fibers, electrical shorting pins, and a streak camera for detonation velocity determination. This provided proven diagnostics for discrete (pins) and continuous (streak) measurement to compare against the CFBG data. Two 85-mm-

long CFBG fibers were glued (M-Bond 200 epoxy) in direct contact along a 7.6-mm-wide facet polished into the charge outer diameter (orange shaded region in Figure 2). A staggered pair of gratings was used since each individual grating was not long enough to span the entire rate-stick length. The end tips of the first and second CFBGs were placed 4.63 and 54.63 mm away from the upstream (initiation) end of the main PBX 9502 charge, respectively. Twelve time-of-arrival electrical shorting pins (Dynasen, Inc., Model CA-1038) were also fielded for comparison with the CFBGs. The pins were located 6.4, 18.85, 31.4, 43.76, 56.7, 69.48, 82.1, 94.92, 107.8, 120.7, 132.82, and 145.42 mm from the upstream end of the PBX 9502 charge. Finally, an imaging streak camera (Cordin Model 132) was used to record position of the detonation front versus time using an external light source to front illuminate the charge. The flat facet of the rate stick in between the CFBGs was polished to allow for specular light reflection from the charge surface. Light from an Argon flash source<sup>18</sup> was then reflected from the flat facet to provide illumination light for the streak camera. The high-luminosity of the explosively driven Argon flash overwhelmed the light emission from the PBX 9502 reaction and product zones. In Figure 3, we plot the data from the two CFBGs. In Figure 3(a), the time recorded raw voltage signals are plotted showing the steady burn of the detonation front as illustrated in the monotonic behavior of the decreasing voltage signals from onset of detonation detection to full consumption of each grating. In Figure 3(b) we plot the recorded data and the calibrated-to-length data after applying the voltage correction curve for the normalized integrated area versus length as shown by the symbol plot in Figure 1(b).

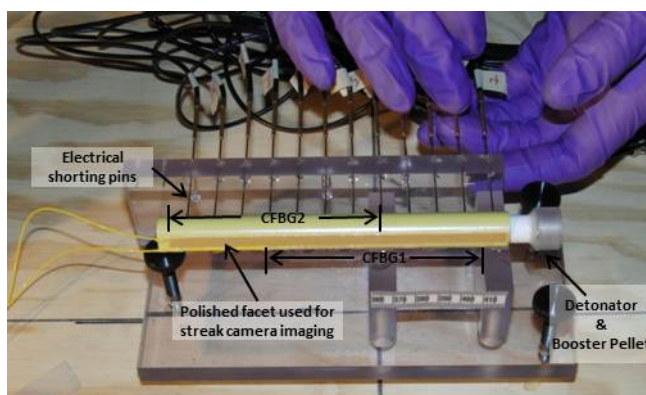


Figure 2. Photograph of PBX 9502 rate stick assembly showing placement of diagnostics: two 85-mm-long CFBGs, 12 electrical pins, and the flat streak-imaging face.

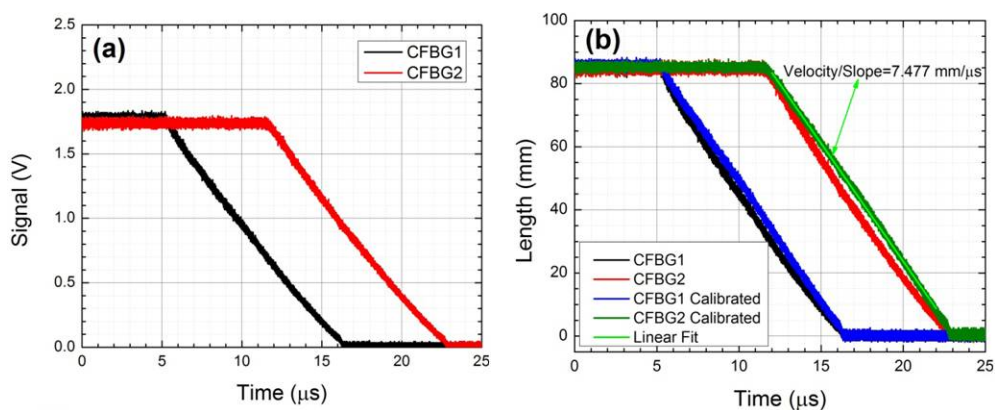


Figure 3. Recorded CFBG data waveforms from PBX 9502 rate stick experiment: (a) raw data voltage versus time traces; (b) traces normalized and calibrated to length. A linear fit to the calibration corrected CFBG2 trace (green curve) in (b) yields a detonation front velocity (*i.e.*, slope) of 7.477 mm/μs.

We compare the CFBG, pin, and streak data by plotting all results together. Figure 4(a) overlays the electrical pin CFBG data. The photograph in Figure 4(b) is a static (top) and dynamic position versus time streak (bottom) of the detonation along the charge. The inset table to Figure 4(a) shows the summary of the extracted velocity for all diagnostics (CFBGs,

pins, streak camera) using a least-squares linear fit for each. The table shows that the CFBG results are within 0.3% of the data from the pins and streak camera. The standard error values in the slope of the linear fits reported as velocity in the table of Figure 4(a) are:  $\pm 0.0010$ ,  $\pm 0.0011$ ,  $\pm 0.0005$ , and  $\pm 0.021$  mm/ $\mu$ s for CFBG1, CFBG2, streak camera, and pins, respectively.

The results from this experiment demonstrate the level of accuracy that can be achieved when steady detonation occurs along a well-defined path. Approaches detailing calibration methods and accuracy are explained in our previous publication.<sup>16</sup> Despite these results, it is still important to understand the sensitivity of CFBG based detonation velocity sensors in situations where variation in detonation velocity from unsteady flow, multiple-HE boundaries, or curved surfaces are involved. We therefore proceeded to establishing baseline experiments where detonation velocity is expected to vary. These experiments are described below.

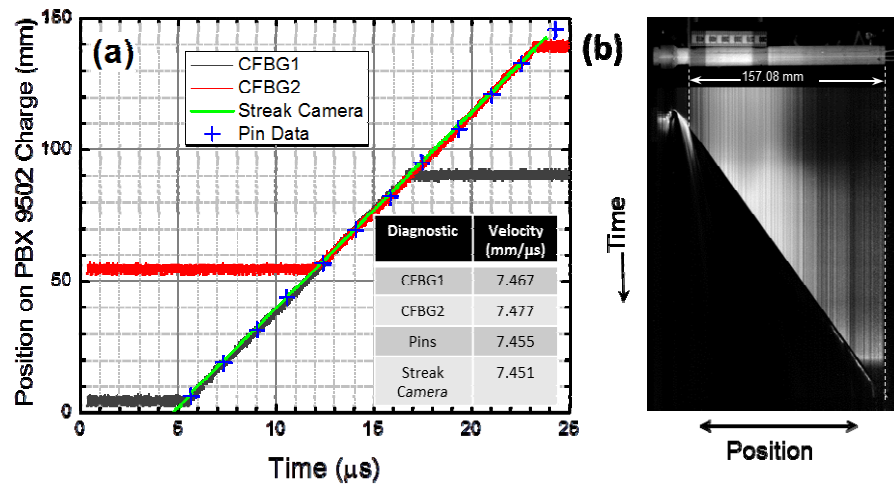


Figure 4. (a) Results of the PBX 9502 rate stick experiment showing a comparison of the CFBG data (red and black curves), the streak camera break out data (green curve), and the electrical pin data (blue crosses). The inset table is the extracted velocity from a linear least squares fit for all three measurements: CFBGs, electrical pins, and streak camera. The standard error values in the slope of the linear fits reported as velocity in the table are:  $\pm 0.0010$ ,  $\pm 0.0011$ ,  $\pm 0.0005$ , and  $0.021$  mm/ $\mu$ s for CFBG1, CFBG2, streak camera, and pins, respectively. (b) Images of the static (top) and dynamic (bottom) streak camera measurement.

### 2.3 Multi-HE Rate Stick

A rate stick test comprised of multiple HE types was used to test the sensitivities of two different CFBGs, each with a different linear chirp rate. The goal was to test spatio-temporal sensitivity effects by combining a measurement where the expected detonation velocity differences (by using different HE materials) can be simultaneously tracked with two CFBG with different linear chirps. In Figure 5 we show an illustration of the HE assembly and the locations of CFBGs fielded. A 12.7-mm-diameter and 154.3-mm-long cylindrical rate stick consisting of five 25.4-mm-long sections of different HE materials (PBX 9501, Comp B, TNT, PBX 9407, PBX 9502) and one 25.4-mm-long section of inert PMMA plastic was fielded for the test. The assembly was initiated by an RP-1 detonator. Test diagnostics included two 100-mm-long CFBGs, five 10-mm-long CFBGs, and a streak camera (Cordin Model 132) for detonation velocity determination. The CFBGs were glued (M-Bond 200 epoxy) at the positions shown in Figure 5, but at different cylinder azimuth angles to minimize for fiber optic cable interferences and for imaging with the streak camera. The 100-mm and 10-mm CFBG spectra are shown in Figures 5(a) and 5(b), and they had a measured chirp of 3.5 nm/mm and 0.35 nm/mm, respectively.

Table 1 below lists the length, position, and material mapping for the seven CFBGs used in the test. The objective is to catalog differences in the performance of the long (100 mm) CFBGs versus the short (10 mm) with respect to the ability to record sudden changes in detonation velocity. The results are shown in Figure 6 for the 100-mm and 10-mm CFBGs.



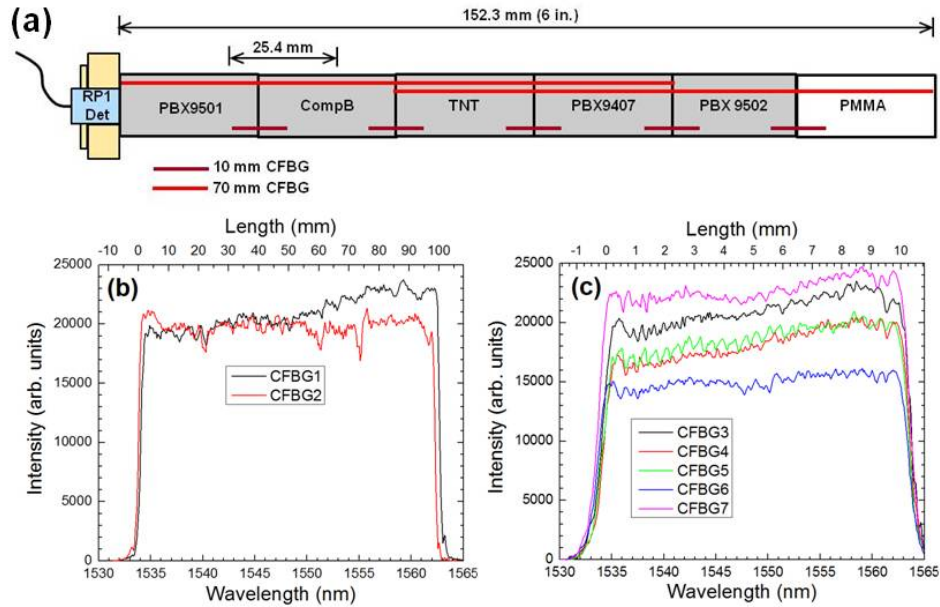


Figure 5. (a) Illustration of the multi-HE rate stick experiment and corresponding CFBG spectra for the (b) 100-mm-long and (c) 10-mm-long sensors. The illustration does not show that the CFBGs had to be placed at varying azimuth angle to minimize fiber optic cabling interference.

Table 1. CFBG sensor lengths, position, and material placement used in the multi-HE rate stick test.

CFBG Sensor	Length (mm)	Position (mm)	Material Interface(s)
1	100	0.54	PBX 9501/Comp B/TNT/PBX 9407
2	100	50.7	TNT/PBX 9407/PBX 9502/PMMA
3	10	20.1	PBX 9501/Comp B
4	10	45.9	Comp B/TNT
5	10	70.7	TNT/PBX 9407
6	10	96.2	PBX 9407/PBX 9502
7	10	121.6	PBX 9502/ PMMA

Comparing the results between two sets shows a slight difference in the ability of CFBGs to detect abrupt changes in slope (velocity) between material interfaces. The 10-mm CFBGs appear to better track the change at the interface as a result of their better spatial resolution, and we can determine that the response time is sub-50 ns to changes in slope. This limit, however, may not be intrinsic to the CFBG detection system, but possibly a function of the disruption in the burn front and material flow across a boundary between different HE materials. For example, for a detonation front traveling at  $7 \text{ mm}/\mu\text{s}$ , in a 50 ns window the front has traveled  $\sim 350 \mu\text{m}$ , and this distance may not sufficient for establishing a steady flow across reactive boundaries. Further tests with faster velocity changes are necessary establish the time resolution limit of CFBGs for detonation velocity measurements. Unfortunately, cross comparison with streak camera measurements were not possible due to failure of the Ar flash system that only partially illuminated the imaging area and resulted in insufficient light for good recording. The streak camera data analysis for partial recovery of the data was not complete yet at the time of this manuscript. Table 2 lists the accepted and measured values for the detonation measurements made in this test. The last column is the experimentally measured averaged detonation velocity as measured by the average of the two 10-mm CFBGs that were placed on each HE. Finally, it also important to briefly highlight the shock velocity as measured in the transition between PBX 9502 and the inert PMMA plastic. The shock

impedance mismatch between the zones accounts for the reduction of the shock velocity launched into PMMA, and demonstrates the CFBG ability to track shock position, provided the shock pressure is high enough to extinguish light return from the CFBG as it travels along the sensor. The ringing in the signal at the near the end of record in the PMMA (Figure 6f) is indicative of an attenuating pressure shock that appears to disrupt the sensor (but not destroy it) after a few mm of propagation into the material.

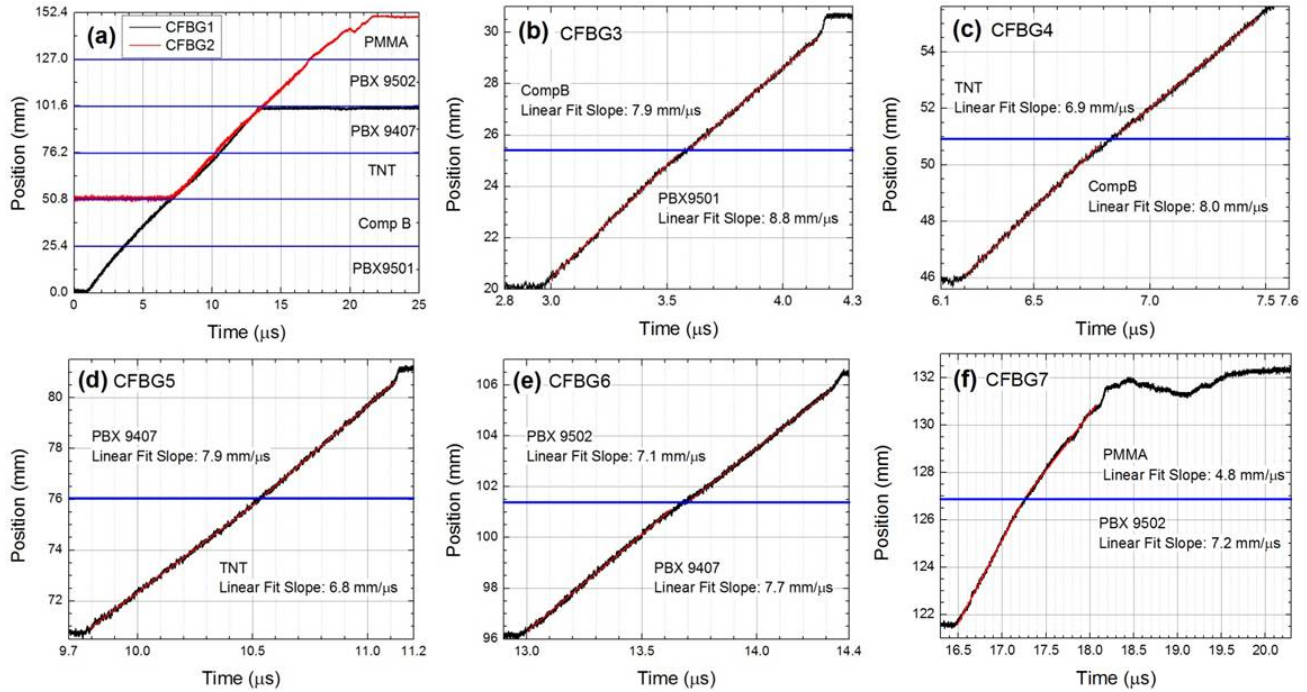


Figure 6. Position versus time results for the multi-HE rate stick test. The two 100-mm-long CFBG results are shown in (a), and five 10-mm-long CFBGs are shown in (b) thru (f). The material boundaries in each plot are designated by a blue colored horizontal line with the material labeled in each section below or above the blue line. Linear fits to data for the 10-mm-long CFBG data are shown as red lines in (b) thru (f), and the slope yielded velocities as labeled in each graph. These are also listed in Table 2. Also note that in (f), a shock wave is launched into the inert PMMA plastic is measured at 4.8 mm/μs.

Table 2. List of the accepted and measured HE detonation velocities used in the multi-HE rate stick test.

HE Material	Detonation Speed (mm/μs)	Avg. Measured Speed with 10-mm CFBG (mm/μs)
PBX 9501	8.8	8.8
Comp B	8.1	8.0
TNT	6.9	6.9
PBX 9407	8.0	7.8
PBX 9502	7.6	7.2

#### 2.4 PBX9501 Detonation along Curvilinear Surface

In the final geometry presented, we demonstrate results from an experiment where the detonation front travels along a meridian line (longitude) in polar coordinates as initiated from the pole in a hemispheric-shaped PBX 9501 HE charge.



The HE charge was tamped on the outside with a tantalum outer metal case, and the CFBGs on the experiment are in between the HE and case and exit the device near the equator. The fibers were laid in a 70-mm-long by 228.6- $\mu\text{m}$  deep groove that was machined into the outer surface of the HE. They were glued (M-Bond 200) in place before the outer metal case was mounted in contact with the HE. An illustration of the placement of two CFBGs in the experiment is shown in Figure 7 showing a full azimuth angle between the gratings of 60 degrees.

Figure 8 shows the results from this hemisphere experiment. The raw data plot in Figure 8(a) demonstrate the excellent simultaneous tracking of the detonation front by the two CFBGs, and the length versus time plot of Figure 8(b) is derived by using the “laser cut method”<sup>15</sup> of calibration as was shown in Figure 5 with excellent linearity between voltage signal versus length/wavelength. The measured detonation velocity in Figure 8(b) is not constant due to the interaction of the radially expanding detonation with the curved explosive charge boundary at the meridian line from near detonator to the flat edge of the charge. To illustrate this point, the green trace in the plot of Figure 8(b) is a tangent line to a linear fit of the CFBG1 data between 5  $\mu\text{s}$  and 7  $\mu\text{s}$  and shows how the beginning and end of the CFBG1 data varies in slope from this tangent line. Figure 9 shows with local linear fits between 2.7  $\mu\text{s}$  - 5  $\mu\text{s}$  (red), 5  $\mu\text{s}$  - 7  $\mu\text{s}$  (green), and 2.7  $\mu\text{s}$  - 5  $\mu\text{s}$  (orange) time slices that the apparent velocity in the front is increasing as the front travels over a recorded run of 70 mm: 8.83 mm/ $\mu\text{s}$ , 9.93 mm/ $\mu\text{s}$ , and 11.0 mm/ $\mu\text{s}$ , respectively.

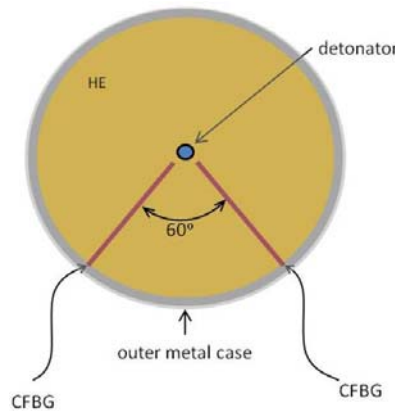


Figure 7. Polar view of experimental diagram showing placement of CFBGs for detonation front measurement in PBX 9501 along a curved meridian (line of longitude). The hemispheric shaped HE charge is contained in an outer metal case, and two 70-mm-long CFBGs are glued between the HE and case. Azimuth angle between the two CFBGs is 60 degrees.

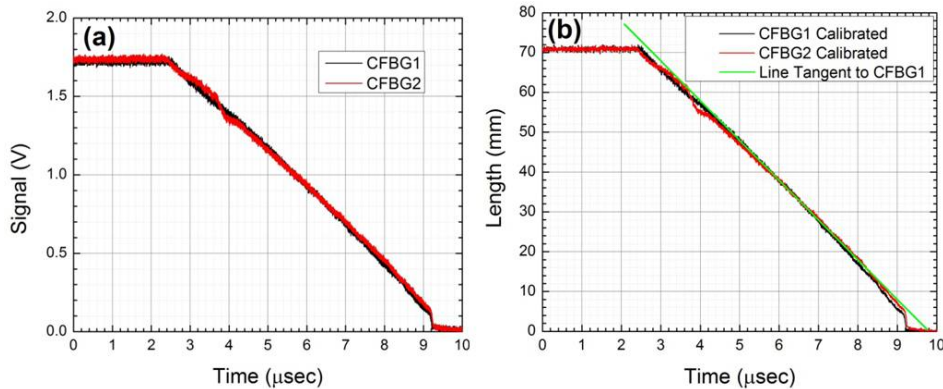


Figure 8. Recorded CFBG data waveforms from PBX 9501 detonation front travels along a meridian line (longitude) in hemisphere detonation front experiment: (a) raw data voltage versus time traces; (b) traces normalized and calibrated to length. The green trace represents an extrapolated line tangent to a linear fit of the CFBG1 calibrated trace between 5  $\mu\text{s}$  and 7  $\mu\text{s}$ . It is used to demonstrate that the phase velocity is not linear.

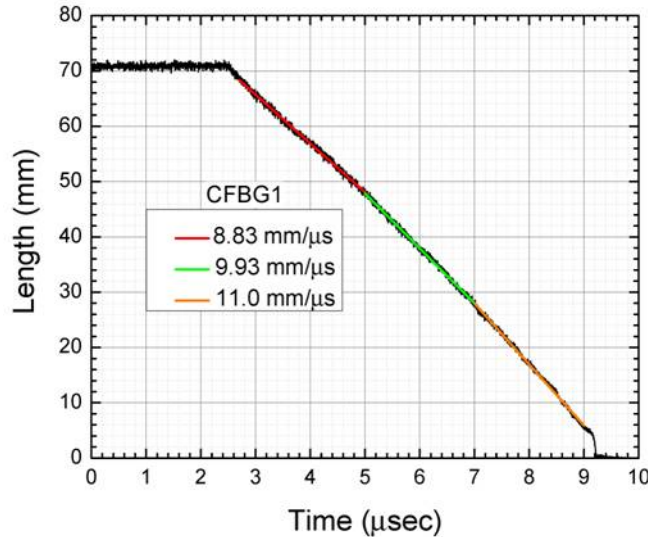


Figure 9. Calculated velocity/slope fits to CFBG data from Fig. 8 show that curvature of hemispheric HE in experiment yields a phase velocity that increases with detonation front as it propagates toward the equator.

### 3. SHOCK PRESSURE MEASUREMENTS

#### 3.1 Experimental Approach

When the shock wave at the detonation burn front (or at a high stress loading condition) does not destroy and consume the Fiber Bragg grating (FBG), the sensor can also be used for thermometry and high pressure wave measurements.<sup>11,12</sup> We have extended initial concept proof studies by Udd, *et al.*<sup>11</sup> in HE deflagration to detonation transition tests to now include using FBG sensors for high pressure shock wave science for flyer plate impact experiments. Initial results for these experiments are described below.

Fiber Bragg grating (FBG) sensors have predictable thermal and mechanical response properties.<sup>8-10</sup> Previously, the wavelength shift of the returning light spectrum has been studied as a function of temperature and applied pressure.<sup>10,19</sup> Under applied pressure, the fiber reflectance spectrum shifts to *shorter* wavelengths, and at elevated temperature, the reflectance spectrum shifts to *longer* wavelength. The pressure and temperature sensitivity shifts of Ge-doped fused silica FBG sensors is measured to be to be  $(d\lambda/dP)(/kbar) \approx -1.9 \times 10^{-4} \lambda$  and  $(d\lambda/dT)(/^{\circ}C) \approx 8.4 \times 10^{-6} \lambda$  ( $\lambda$  in nm).<sup>20</sup> So for a pressure wave to 100 kbar, a spectral shift of 30 nm at  $\lambda=1550$  nm to the blue in the return FBG spectrum is expected and a shift of 6.5 nm to the red is expected at  $T=500^{\circ}C$ . The linear response of the FBG reflectance peaks to pressure was demonstrated up to  $\sim 1$  kbar in hyperbaric chamber tests.<sup>11</sup> Recently, the dynamic response of a FBG was validated with a field test in a deflagration-to-detonation transition tests at the ATK Aerospace Systems test site in Utah.<sup>11,12</sup> Peak dynamic pressures and temperature to  $\geq 80$  kbar and  $400^{\circ}C$  were measured. To date, only a few FBG proof tests exist for either high pressure and/or high temperature. Therefore, it should be possible to simultaneously measure temperature and pressure from a FBG sensor if wavelength dependent shifts in the return spectrum from a FBG sensor can be decoded from the return signal for detection. One approach would be to spectrally disperse the return light signal from a FBG and then have spectral channels read out by an InGaAs linear detector array for light sources about 1550 nm. However, the fastest readout speeds of commercial InGaAs are too slow (state-of-art currently approaching 50 kHz for a 1024 element diode array) to capture spectral shifts from FBG sensors for high-speed dynamic events that are often on the sub-microsecond timescale. Instead, our approach consists of a set of single element InGaAs photodetectors in series with in-line fiber optic spectral filtering methods to encode wavelength shifts into intensity modulation on the output of the return signal. In addition, we also use a specialty uniform fiber Bragg gratings in side-hole fiber (SH-FBG) as the pressure sensor because its polarimetric response results in a pressure-dependent splitting of the 1550 nm reflectance peak that is principally temperature independent and previously measured to be  $-0.66$  nm/kbar.<sup>11,21</sup> In Figure 10, we illustrate our experimental setup. The ASE C-band light source and circulator are the same as those used in the detonation velocity detection system of Figure 1(a). The SH-FBG is a few-mm-long uniform (non-chirped) grating



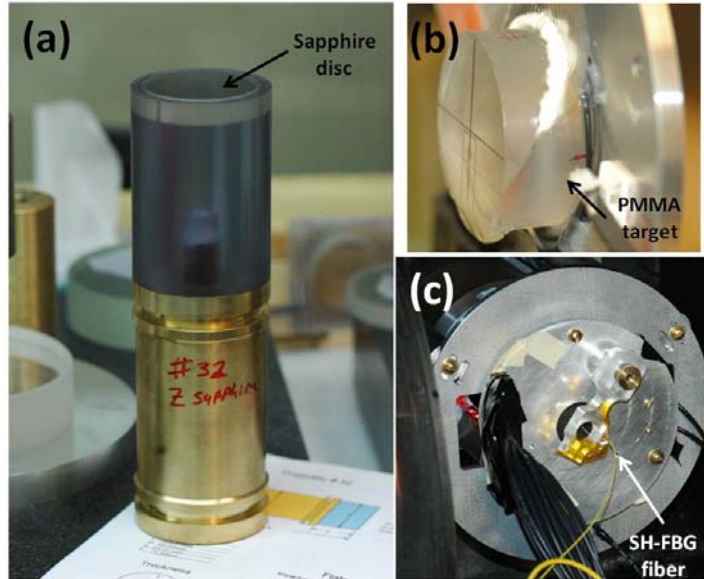


Figure 11. Photographs of the various parts for the PMMA plate impact experiments: (a) sapphire impactor before insertion into gas gun; (b) PMMA target cylinder is comprised of two wedges to allow for insertion of particle velocity gauges at various positions in the sample; (c) assembled PMMA target inserted into catch tank of gas gun showing the center location where the SH-FBG sensor is placed.

( $t_0$ ,  $t_1$ , and  $t_2$ ) under pressure loading from the shock wave, the SH-FBG spectrum will split into two peaks. The shorter wavelength peak will move across the intensity notch filters going through maxima and minima in the spectrum. This information is imparted to the total return signal as modulation as measured by the photodetectors. In Figure 12(c), we show the data recorded in 14 kbar test. The black trace in Figure 12(c) is the SH-FBG signal as recorded by the reference channel where there are no filters. First note that the signals from all channels last only 600 ns. This is consistent with a high pressure shock wave traveling at a few mm per  $\mu$ s and is approximately the transit time along the entire length of the grating,  $\sim 3$  mm. The black curve is also observed to increase with time, by a about a factor of 2.5. This is interpreted as a result of the spectrum from the SH-FBG splitting into two peaks and increasing the integrated light return signal from the addition of the second peak. The red and blue curves in Figure 12(c) are the SH-FBG signals from the channels going through the coarse and fine intensity notch filters, respectively. The red curve clearly shows at least two maxima and possibly three. Two maxima in the coarse filter channel, corresponds to a wavelength of approxi-

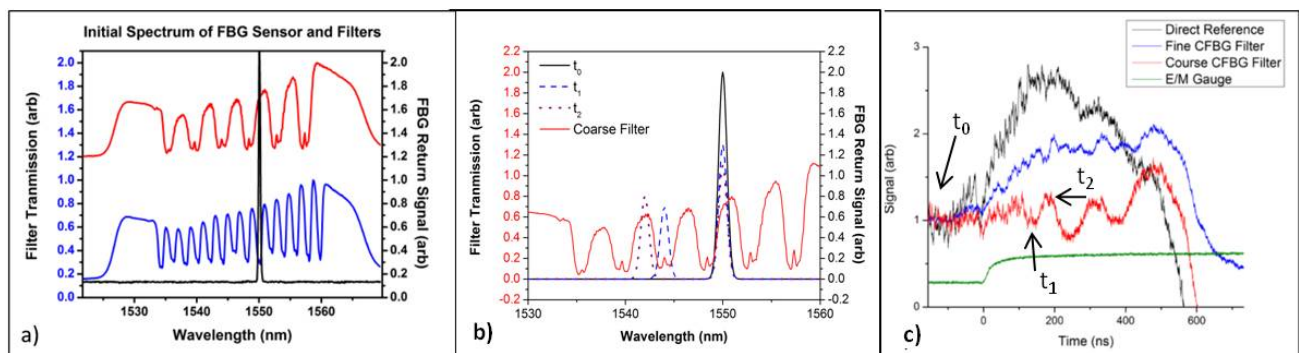


Figure 12. Graphs illustrating the various spectral response data from a SH-FBG pressure measurement diagnostic for shock wave pressure measurements. The static SH-FBG spectrum is shown in (a) with the coarse and fine notched filter channels used to encode the signature of spectral shifts on the intensity return signal as illustrated in the diagram of Fig.10. In (b), upon pressurization at various increasing pressure and time points ( $t_0$ ,  $t_1$ ,  $t_2$ ), the SH-FBG responds by peak splitting and shifting its bluest peak to shorter wavelengths and sliding across the notched coarse filter spectrum to produce modulations in the sensor reflected intensity as light return signal is transmitted for detection. In (c) the data from a 14 kbar gas gun test shows the recorded pressure in the PMMA target.

mately 10 nm. The expected shift for a 14 kbar pressure wave is  $\sim 9.2$  nm. The blue curve data in Figure 12(c) is the channel with the fine filter. For a 10 nm shift, at least five oscillations are expected, however, this is difficult to see based on the signal-to-noise in the blue curve data. There does appear to be multiple oscillations this is consistent with what would be expected. The green curve is the data from the particle velocity gauge, and its time signature is consistent with the recording from the SH-FBG sensor. In just these preliminary data we observe that FBGs hold promise as a high pressure diagnostic for shock wave science. We are currently performing upgraded modifications to our system to improve our signal-to-noise and wavelength selection technique for better decoding of wavelength shifts for our next set of tests.

#### 4. SUMMARY

Experiments at Los Alamos show that FBG sensors are being developed and deployed for use in high explosive and shock wave science experiments. In the case of high explosive detonations, success is demonstrated for several important tests where linearly chirped fiber Bragg gratings are used to measure detonation front position versus time in linear and curvilinear geometries. In a carefully calibrated test, we show that a detonation along a single-HE linear rate stick accuracy to the 0.3% level is achieved when compared with other methods. In the detonations involving multiple-HE materials, we show that gratings with larger chirp rates have better sensitivity to changes in velocity. The results for 10-mm (chirp: 3.5 nm/mm) gratings compared to 100-mm (chirp: 0.35 nm/mm) gratings show that changes in velocity are better tracked (sub-50 ns) by the 10-mm gratings because of the better spatial resolution than the 100-mm gratings. However, the fastest time resolution is still yet to be determined as the tests conducted have not tested the ultimate limit of the grating or detection system. In addition to detonation, we also have begun studying the response of fiber Bragg gratings to high pressure produced by shock waves in gas gun driven plate impact experiments on PMMA targets. In particular, specialty uniform side-hole fiber Bragg gratings were used to develop a pressure diagnostic that can be used as in-situ shock physics experiments. Preliminary results using a 3 mm long side-hole fiber Bragg grating in experiments between 6 and 20 kbar impact-target tests on PMMA demonstrate that pressure induces a frequency shift on the return signal consistent with expected response from a side-hole fiber Bragg grating. Our results for the 14 kbar tests show that such measurements are feasible, and that system improvements are necessary to increase the fidelity of the pressure measured. We are currently refining our signal detection to include improving signal-to-noise and wavelength encoding/decoding that we hope to report on soon after our next set of tests.

#### ACKNOWLEDGEMENTS

Funding for this work was provided by the Gemini Project and the Campaign 2 "High Explosive Science" Program at Los Alamos National Laboratory under the auspices of the Department of Energy for Los Alamos National Security LLC under Contract no. DE-AC52-06NA25396. The authors also thank the Center for Integrated Nanotechnologies, Los Alamos National Laboratory for providing access to their ultrafast laser machining facility to cut and calibrate the fiber Bragg gratings used in this work. E. Udd, President of Columbia Gorge Research, LLC is supported under the Department of Defense Phase II SBIR contract W31P4Q-11-C-0209 from the U.S. Army.

#### REFERENCES

- [1] Bdzil, J. B. and Stewart, D. S., "Modeling two-dimensional detonations with detonation shock dynamics," *Phys. Fluids A* 1(7), 1261-1267 (1989).
- [2] Lambert, D. L., Stewart, D. S., Yoo, S., and Wescott, B. L. "Experimental validation of detonation shock dynamics in condensed explosives," *J. Fluid Mech.* 546, 227-253 (2006).
- [3] Bancroft, D., Peterson, E. L., and Minishall, S., "Polymorphism of iron at high pressure," *J. Appl. Phys.* 27(3), 291-298 (1956).
- [4] Barker, L. M., Shahinpoor, M., and Chhabildas, L. C., [High-Pressure Shock Compression of Solids], "Experimental diagnostics and techniques", New York, Springer-Verlag, 43-73 (1993).
- [5] Duvall, G. E., [Shock Waves in Condensed Matter], "Shock wave research: yesterday, today, and tomorrow," New York and London, Plenum Press, 1-12 (1986).
- [6] McCall, G. H., Bongiovanni, W. L., and Miranda, G. A., "Microwave interferometer for shock wave, detonation, and material motion measurements," *Rev. Sci. Instrum.* 56(8), 1612-1618 (1985).

- [7] Strand, O., Hare, D., Garza, R., Whitworth, T. and Holtkamp, D., [Proceedings of the 14th International Detonation Symposium], "Embedded fiber optic probes to measure detonation velocities using the photonic doppler velocimeter," Office of Naval Research, Arlington, VA, 401 (2010).
- [8] Jewart, C. M., Wang, Q., Canning, J., Grobnic, D., Mihailov, S. J., and Chen, K. P., "Ultrafast femtosecond-laser-induced fiber Bragg gratings in air-hole microstructured fibers for high-temperature pressure sensing," *Opt. Lett.* 35(9), 1443-1445 (2010).
- [9] Zhang, B., and Kahrizi, M., "High-temperature resistance fiber Bragg grating temperature sensor fabrication," *IEEE Sens. Journ.* 7(4), 586-591 (2007).
- [10] Mihailov, S. J., "Fiber Bragg grating sensors for harsh environments," *Sensors* 2012 12(2), 1898-1918 (2012).
- [11] Udd, E. and Benterou, J., "Improvements to high-speed monitoring of events in extreme environments using fiber Bragg grating sensors," *Proc. SPIE* 8370, 83700L (2012).
- [12] Udd, E., [Proceedings of JANNAF], "Innovative very high speed fiber grating sensor system to characterize explosives and propellant," Chemical Propulsion Information Agency Center, Columbia, MD, (2012).
- [13] Benterou, J., Bennett, C. V., Cole, G., Hare, D. E., May, C., Udd, E., Mihailov, S. J., and Lu, P., "Embedded fiber optic Bragg grating (FBG) detonation velocity sensor," *Proc. SPIE* 7316, 73160E (2009).
- [14] Udd, E., Benterou, J., May, C., Mihailov, S. J., and Lu, P., "Review of high-speed fiber optic grating sensor systems," *Proc. SPIE* 7677, 76770B (2010) .
- [15] Rodriguez, G., Sandberg, R. L., McCulloch, Q., Jackson, S. I., Vincent, S. W., and Udd, E., "Chirped fiber Bragg grating detonation velocity sensing," *Rev. Sci. Instrum.* 84(1), 015003 (2013).
- [16] Sandberg, R.L., McCulloch, Q., Dattelbaum, A.M., Staggs, K.W., Rodriguez, G., [2012 Conference on Lasers and Electro-Optics (CLEO)], "Nondestructive calibration of chirped fiber Bragg grating sensors using a fiber-based ultrafast laser," *Optical Society America, Washington, DC, AW3J.2* (2012).
- [17] McCulloch, Q., Sandberg, R. L., Dattelbaum A. M., Staggs, K. W. and Rodriguez, G., [Lasers, Sources, and Related Photonic Devices, OSA Technical Digest], "Fiber-based ultrafast laser fabrication system with application to chirped fiber Bragg grating sensors," *Optical Society America, Washington, DC, JTh2A.24* (2012).
- [18] Davis, W. C., Salyer, T. R., Jackson, S. I., and Aslam, T. D., [Proceedings of the 13th International Detonation Symposium], "Explosive-driven shock waves in argon," Office of Naval Research, Arlington, VA, 1035-1044 (2006).
- [19] Frazao, O., Ferreira, L. A., Araujo, F. M., and Santos, J. L., "Application of fiber optic gratings technology to multi-parameter measurement," *Fiber and Integrated Optics* 24, 227-244 (2007).
- [20] Rao, Y.-J., "In-fibre Bragg grating sensors," *Meas. Sci. Technol.* 8(4), 355-375 (1997).
- [21] Wu, C., Li, J., Feng, X., Guan, B.-O., and Tam, H.-Y., "Side-hole photonic crystal fiber with ultrahigh polarimetric pressure sensitivity," *J. Lightw. Technol.* 29(7), 943-948 (2011).